euronoise 2021
25th to 27th of October
Madeira, Portugal - online

Computational design applied to small room acoustics: creating and evaluating custom solutions

Valentijn Bors[1], **Sebastiaan Bors**[2]

[1]Amsterdam University of Applied Sciences
v.t.b.bors@hva.nl
[2] sebastiaan.bors@gmail.com

Abstract
This paper evaluates a design procedure which is able to scale one-dimensional quadratic-residue diffusers, with integrated Helmholtz resonators. These acoustic structures can be tuned to room modes while fitting within a specified volume. An algorithmic solver is used to control geometric parameters in order to achieve a target frequency. The effect of the diffuser on a room is estimated using Pachyderm. Values obtained with simplified models, that make use of analytically derived coefficients, are compared with those obtained by simulating the full geometry. The predictive power of the simplified modeling made it preferable over simulating the full geometry in comparable scenarios. CFD simulations and measurements taken from a 1:1 scale prototype, are used to evaluate the applicability of lumped mass models to predict resonance frequency and absorption of slit Helmholtz resonators. Although the obtained results remain inconclusive, they indicate a higher inertial attached length for semi-infinite slit resonators, than typically found in literature. If these results can be validated, then the procedure should provide reliable designs.

Keywords: Helmholtz resonators, QRD, CFD, Pachyderm, parametric

1 Introduction

Small rooms provide unique challenges for any acoustic treatment, as each room is different in their acoustical behaviour, and the space available for acoustic treatment is often limited. Computational design procedures could be used to efficiently shape and evaluate customized retrofit solutions within relatively short time frames. These design and automation principles are applied to a case study in an effort to evaluate the feasibility of these notions. Figure 1 shows a small room used for music production which is used as a test case. A section of the back wall is available for acoustical treatment, referred to as volume L. The acoustical treatment, used in this study, is meant to solve two common problems in small room acoustics: low frequency room modes and coloration due to specular reflections. The proposed treatments are one-dimensional quadratic-residue diffusers (QRDs) with integrated Helmholtz resonators tuned to specific room modes, as their characteristics are well-known and quantifiable through semi-analytical models. This also enables the use of simplified geometries by applying derived coefficients to larger surfaces instead of requiring detailed and extensive acoustical simulations. While volume L could theoretically be filled by a singular QRD, this would be relatively difficult to manufacture due to potential size. Instead, the QRD is recommended to consist of multiple *elements* that can be populated within volume L. The design procedure and the structure tailored for this test case are discussed in section 2. Sections 3 and 5 detail the tuning of the QRDs and their effect on the room using Pachyderm Acoustics (v2.0.0.2.), an acoustics simulation plugin for Rhinoceros 3D and Grasshopper. The modeling of the

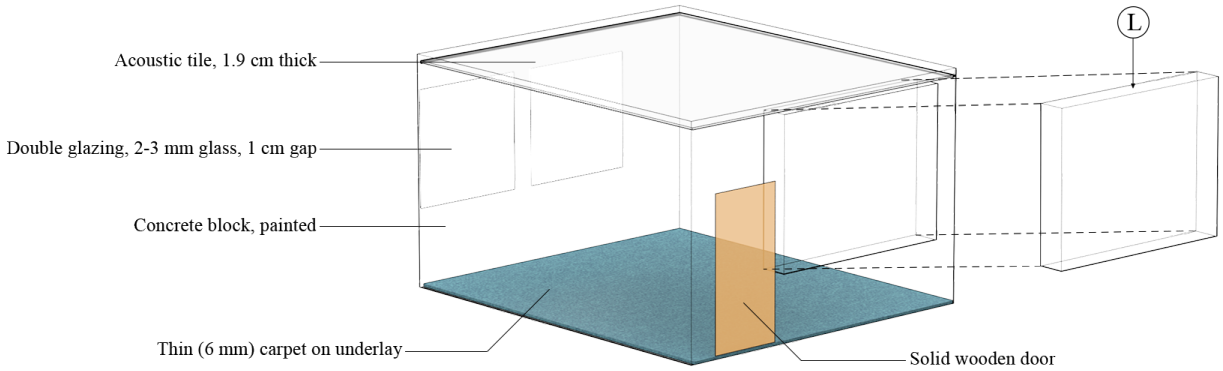

Figure 1: Testcase studio ($5.15m \times 4.36m \times 2.97m$), where L is available for treatment ($2.56m \times 1.98m \times 0.30m$).

integrated resonators by way of lumped mass models (LLM) is described in section 4. In an effort to evaluate these methods a multitude of computational fluid dynamic (CFD) simulations have been carried out in addition to acoustical experiments on a physical prototype in a reverberation chamber.

2 Design procedure

The proposed design procedure, as shown in figure 2, is able to scale a 1D QRD with two integrated slit Helmholtz resonators according to various inputs. First, the dimensions of the room are given in order to obtain the target frequency for the Helmholtz resonators. It is assumed that low frequency room modes are to be absorbed as they are a potential problem in small rooms. This is because the modal density in low frequencies is much smaller [1]. For rectangular rooms, the modes can be approximated using equation 1,

$$F_n = \sqrt{\left(\frac{a_n}{L}\right)^2 + \left(\frac{t_n}{W}\right)^2 + \left(\frac{o_n}{H}\right)^2} \tag{1}$$

in which F_n is the resonant frequency, c is the constant of the speed of sound, a_n is the axial room mode number, t_n is the tangential room mode number, o_n is the oblique room mode number, and L, W and H are room dimensions in meters. The second input selects which room mode is to be absorbed. For the test case, its third axial mode of $100Hz$, is selected as the target frequency. The third input defines the space, volume L, that is available for the acoustic treatment and consequently the maximum dimensions of each QRD. The prime number defines the amount of wells per QRD. The material thickness defines the width of the dividers,

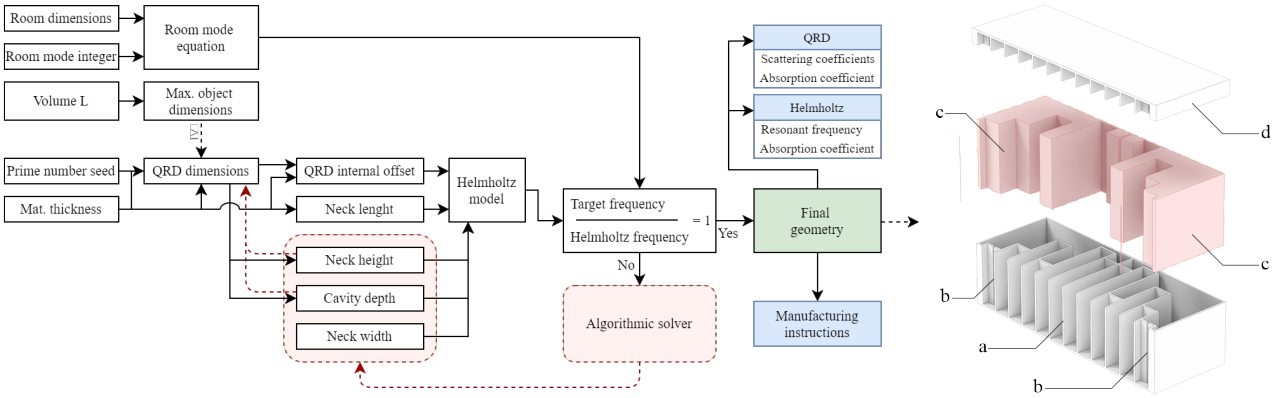

Figure 2: Left: design procedure. Right: exploded view of resulting geometry, where a) is a N13 1D QRD, b) are the slits of the Helmholtz resonators, c) are the cavities of the resonators, and d) is the top of diffuser. The overall dimensions are $0.83m \times 0.30m \times 0.24m$ with a wall thickness of $8mm$.

the internal offset within the QRD which in turn creates the cavity of the Helmholtz resonators, and defines their neck length. This leaves the neck width as the last input to be defined which can be accomplished via algorithmic solvers by setting its target solving value, as a result of dividing the target frequency by the achieved frequency, to 'one'. The choice of the algorithmic solver is crucial as it can have significant impact on the results obtained [2]. The design procedure has the final geometry as an output, as depicted in figure 2, with the relevant corresponding scattering coefficients, absorption coefficients and resonant frequencies. Methods used to obtain these parameters are discussed in section 3 and 4. Manufacturing instructions can be obtained by dividing the geometry into different panels that could be milled or laser-cut. Alternatively, an inner curve can be generated to be used as a trace curve for large scale 3D printing end effectors. As these instructions vary immensely per production technique and even machine, they will not be further detailed within this paper. During this study, the design procedure was defined as a Grasshopper script, utilizing the Galapagos solver.

3 Quadratic residue diffusers

The QRD is designed according to principles derived from Cox and D' Antonio [3]. The thickness of the dividers can be any as long as they are rigid and reasonably thin. The depth of each well is defined in accordance to equation 2, which describes the relationship between the depth d_n as a result of a quadratic residue sequence $S_n = n^2 mod\ N$, the wavelength of a frequency λ_n, and prime numbers N. The first well is divided in half with one half placed on each side of the QRD in order to ensure symmetry.

$$d_n = \frac{S_n \lambda_n}{2N} \tag{2}$$

Given a maximum depth, it is possible to calculate the natural frequency (f_0) using equation 3,

$$f_0 = \frac{cS_{max}}{2Nd_{max}} \tag{3}$$

in which c is the speed of sound and S_{max} the largest number in the quadratic residue sequence. An estimation of the scattering coefficient can then be carried out in accordance to equation 4,

$$s' = 1 - \left| \frac{1}{N} \sum_{n=1}^{N} e^{-2jkd_n} \right|^2 \tag{4}$$

where the wave number k equals ω/c. Note that this model is not ISO compliant but it has proven to be surprisingly accurate and its numerical approach enables it to be integrated within the design procedure [3]. The behavior of the scattering coefficient at different frequencies is shown in figure 3. A QRD can absorb sound by virtue of their material, the presence of thermal and viscous boundary layers and other effects not discussed here. Absorption coefficients can be approximated by accounting for the presence of thermal and viscous boundary layers, while assuming smooth walls [4]. Equation 5 can be used to approximate the absorption coefficient.

$$\alpha = 1 - \left| \frac{z-1}{z+1} \right|^2 \tag{5}$$

This requires the determination of the dimensionless impedance, z, at the entrance of each well,

$$z_n = -i \left\{ 1 + (1-i) \frac{\delta_v - (\gamma - 1)\delta_h}{2b_n} \right\} cot(k_t d_n) \tag{6}$$

where, γ is the impressibility ratio of air. The thicknesses of the viscous and thermal boundary layer can be determined using $\delta_v = \sqrt{2\nu/\omega}$ and $\delta_h = \sqrt{2\chi/\omega}$ respectively. Here ω is the radial excitation frequency, ν and

χ are the kinematic viscousity and thermal diffusivity of air and k_t is the propagation number which can be approximated with equation 7.

$$k_t \approx k + \frac{k}{2b_n}(1-i)[\delta_v + (\gamma-1)\delta_h] \tag{7}$$

Both the obtained and expected absorption of the QRD well are fairly small, due to the large well widths. Below 8000Hz the estimated absorption coefficient remains below 0.01. The choice of well width is based on minimal high frequency absorption and lower ray tracing requirements, as discussed in section 5. In reality, these values are proven to be typically higher and depend on the material the QRD is constructed with and its surface qualities [5]. Both of the aforementioned studies acknowledge that a more accurate analytical model has yet to be developed. The obtained scattering coefficients and absorption spectra can be used to aid the ray tracing simulations which is also discussed in the next section.

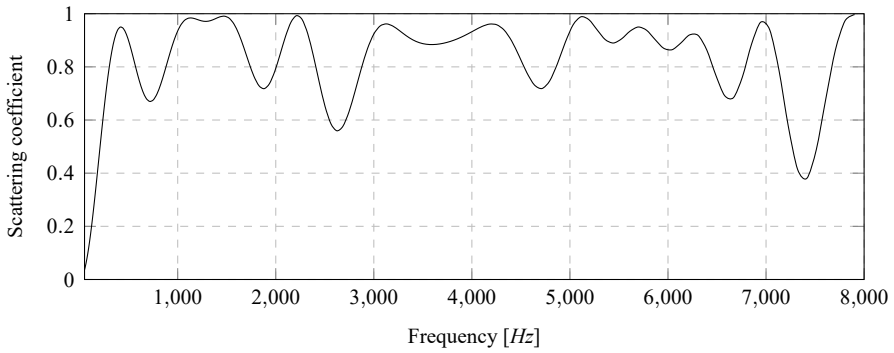

Figure 3: Predicted scattering coefficients of the QRD

4 Helmholtz resonators

An accurate prediction of the resonant frequency of the integrated Helmholtz resonators is an essential component in the design procedure as it should target specific frequencies. The ability to predict the absorption characteristics given a range of frequencies with some accuracy, is useful in evaluating the effectiveness of the resonators and whether they are worth incorporating in any specific design. The geometry used for this paper incorporates two slit resonators, with separate cavities in order to suppress lateral propagation. Both resonators feature an irregular shaped cavity defined by an internal offset of the outer geometry of QRD. The neck and cross-sections are rectangular with a height equal to that of the cavity and a length equal to the material thickness. No porous absorbent is applied. Modeling the natural frequency and absorption characteristics of a Helmholtz resonators is typically performed with a linearized lumped mass model (LLM). These models are varied, accounting for different geometric or physical effects. This study will use a model that should be able to account for thermal and viscous (boundary layer) effects [6]. The model needed only a small adaption to account for the difference in topology as discussed later. The model equations have been rewritten in a compacted form for the sake of brevity. The corrected natural frequency ω_{0k}, in rad/s, can be obtained using equation 8,

$$\omega_{0k} = c\sqrt{\frac{S_0}{V\left[l_0\left(1+\frac{2\delta_v}{d_0}\right)+l_a\right]}} \tag{8}$$

in which S_0 is the cross-sectional area of the neck and V is the volume of the resonator. The term between square brackets represents the effective length of the neck which is corrected for the presence of boundary layers. l_0 is the physical length and d_0 is the width of the neck. l_a is the inertial attached length, or end correction. Given that the geometry of the resonator used in this study contains a very high and narrow slit, the expression derived [7] and used by Komkin [6] is not likely to yield accurate results as it applies to cylindrical resonators or rectangular

resonators with similar cross-sectional areas. Numerous alternative expressions concerning the attached length for orifices have been devised by either derivation, experiment or numerical simulations. These often build upon the foundational works of Rayleigh [8] and Ingard [9]. After conducting a comprehensive survey of many existing models a unification has been introduced by Jaouen et al. [10]. Reyleigh proposes that the inertial attached length will be between $\pi r/4 < l_a < 8r/(3\pi)$, where r is the radius of the orifice. Ingard also considered rectangular neck topologies, however these seem not applicable to slots with very high neck heights. For a two-dimensional or semi-infinite case, the attached length would keep increasing indefinitely with the square root of the height of the neck. To the authors knowledge, there is no definitive source on inertial attached lengths for slit resonators with semi-infinite heights. Eventually, Reyleigh's $l_a \approx 0.82 d_0$, approximation was used based on the work of Durá et al. [11], as their model reduces to that approximation given the current topology. A slight reduction in frequency is likely due to the asymmetry of the cavity, however given the size of the cavity and the local similarity of the topology, the shift in frequency should remain small [12]. In order to compare the predictive power of the LLM model with the CFD simulations and experimental data, an absorption spectrum will be constructed. The absorption coefficient can again be obtained using equation 5 and the dimensionless impedance as shown below,

$$z = \frac{S}{S_0}\left[2k\delta_v\left(\frac{l_0}{d_0}+\varphi\right)+\frac{S_0 S_s \delta_h}{kV^2}\right]+i\frac{cS}{V}\left(\frac{\omega}{\omega_{0k}^2}-\frac{1}{\omega}\right) \tag{9}$$

where S is the cross-sectional area of the QRD and S_s is the surface area of the cavity. φ is an empirically derived corrective factor that approximates the additional neck length as a result of the viscous losses that occur at the edges of the neck. Appropriate values ranging between 1 and 1.13 can be used [6]. A value of 1.13 is used throughout this study. Note that the equation above does not reflect the proper scaling due the presence of two decoupled resonators. The resulting absorption spectrum is depicted in figure 6, where a second curve shows the absorption characteristics without the correction for viscous and thermal effects.

5 QRD modeling using Pachyderm

In order to estimate the effect of the diffuser has on the room of the test case, three scenarios were simulated using Pachyderm. First, the current room without the diffuser. Second, the diffuser modeled as volume L with scattering- and absorption coefficients applied to its room facing surface. These coefficients are obtained as discussed in section 3. Third, the diffuser fully modeled as the final geometry populated 24 times, in order to fill volume L. A "smooth" material applied is applied in this last case. Though the analytical models assume perfectly smooth walls, the smooth material in Pachyderm is given a scattering- and absorption coefficient of 0.01 across the frequency spectrum to prevent a ray from potentially bouncing between walls indefinitely. Other material properties were assigned according to values derived from Cox & D'Antonio, as shown in figure 1. As Pachyderm expects values for $62.5Hz$ and $8000Hz$, the values used are the same as $125Hz$ and $4000Hz$ respectively. Note that Pachyderm is currently unable to simulate singular frequencies, so any potential effect of the Helmholtz resonators is not accounted for in these simulations.

The simulations were carried out using the image source method set to one image order, combined with ray tracing. The number of rays doubled per simulation, starting at 125 rays up to, and including, 8000 rays. A cut-off time of $2000ms$ was enforced. Environmental factors included an air temperature of $20°C$, relative humidity of 50%, and an air pressure of 1000 hPa. The ISO 9613-1 (Outdoor Attenuation) method was used. Within the room two omnidirectional sources, representing loudspeakers, were placed at $1m$ from the back wall and $1m$ and $3m$ distance from the sidewall respectively. Both sources emit $120SWL$ across the frequency bands. A receiver was placed centered within the room. The simulations were run on a system that utilizes an Intel i7-6700HQ CPU which runs at $2.60GHz$, and $31.8GB$ of RAM. Pachyderm can also be used within Grasshopper during an iterative process where an algorithmic solver can be used to obtain a target value. This process would require various cycles of calculations where a relationship between accuracy and computational time needs to be established. The obtained results are discussed in section 8.

6 Resonator modeling using CFD

Numerical investigation into the absorption behavior of the resonator-diffuser combination within the context of the room was performed using rhoPimpleFoam, a transient, compressible finite volume solver. Changes in density, temperature and enthalpy are accounted for using the energy equation. Air was assumed to be an ideal gas at 296 Kelvin. Fluid turbulence was modeled using the LES WALE method. The computational domain consisted of a two-dimensional slice of the studio, as shown in figure 1, using a square grid, with a total of $79.6 \cdot 10^4$ cells. Grid resolution ranged from 0.04 to 8mm, with 50 cells spanning the width of the resonator neck. The average resolution within the cavity and at the diffuser walls were 1mm and 2mm respectively. The mesh got progressively coarser with increasing distance from the resonator. A small grid convergence study has been carried out to ensure that size limit of 8mm would not be too diffusive for the pressure waves. No noticeable deviations in wave characteristics were observed at this resolution with respect to finer grids. The (subgrid) turbulent viscosity ratios observed were below 10^{-5}, indicating sufficient grid resolution for the amount of turbulence present in the system. y^+ values in the neck remained below 0.25, which also indicates sufficient resolution in the wall normal direction. In order to excite the resonator at a range of frequencies a ”chirp” sound was ”played” which created an oscillating pressure boundary condition. The source of the pressure waves, located at the far side of the studio, was modeled as a velocity inlet-outlet with a fluctuating pressure boundary condition. This is not strictly physical, but sufficient for the scope of these simulations. The width of this ”speaker” equals that of the QRD geometry. The pressure would oscillate around $10^5 Pa$, with a frequency of $40 + 20t$ Hz and an amplitude of $5.6Pa$. Due to time constraints the simulation was halted after 4.5 seconds, which means that the range of frequencies at the ”speaker” was 40 to 130Hz. However, higher frequency waves were present at the resonator neck by virtue of wave interactions. In order to fill in the frequency spectrum further, additional simulations have been carried out at 78, 100, 156, 221 and 312Hz. Their time span was defined by a minimum of 20 periods and an additional 0.14 seconds. Marching through time was carried out by utilizing implicit Crank-Nicolson time integration. The upper limit on the time step size was defined as $min(4 \cdot 10^{-4}/(\pi\omega_i), 2 \cdot 10^{-5})$, where ω_i is the excitation frequency. This should allow enough resolution to capture the pressure waves and any large eddies that might be present. The timestep was automatically reduced if the Courant number exceeded 0.5. A maximum of 10 outer iterations was set for each time step. Almost all time steps converged with 4, and sometimes 7 iterations to a relative tolerance of 10^{-3} or an absolute residual below 10^{-6} for all fields. The described numerical setup is likely over-resolved, meaning that any discrepancies with respect to the physical world will be mostly due to the two-dimensional reduction. This limits the accuracy of the turbulence modeling and the choice of boundary conditions instead of discretization or modeling errors.

7 Prototype testing

A prototype of the design was made from 8 and 4mm thick medium-density fibreboard with individual panels cut out by a laser cutter. The panels were joined together using glue. Internal borders were treated with a polymer-based sealant to prevent leaks. Only one significant deviation from the design to the tested geometry was found. Close inspection revealed that one of the panels defining the neck of the second Helmholtz resonator shifted by 0.7mm. This effective reduction in neck length could lead to a 12Hz increase (according to the corrected LLM model) in resonance frequency for that specific resonator. This is likely the main cause of the difference in resonant frequency between the measurements and CFD results as discussed in section 8. The prototype was tested in a reverberation chamber. The chamber had a receiving volume of $220.8m^3$, an internal temperature of $24°C$, a relative humidity of 49%, and a pressure of $103.1kPa$. Using an omnidirectional speaker, the room was excited with 100dB white noise for eight seconds after which the reverberation time values per third octave bands were measured. Five scenarios were considered, first the empty room, where three microphone positions and nine impulses per position were used. Second, the room with the prototype, using nine encircling microphone locations and three impulses per position. The individual resonators were tested by placing the microphone at the necks of each resonator respectively. The fifth scenario has the microphone at 1m distance from the surface, on the symmetry plane as shown in figure 4d. Nine impulses were used for each position.

(a) Chamber. (b) Near resonator 1. (c) Near resonator 2. (d) At 1m distance.

Figure 4: Impression of microphone placements within reverberation chamber.

8 Results

Ascertaining the effectiveness of Pachyderm and the use of simplified QRD models therein, has been attempted by simulating three scenarios as discussed in section 5. Figure 5a shows the 15dB reduction reverberation times for different frequency ranges. The inclusion of the QRD increases the T_{15} values frequency ranges below 1000Hz. This increase becomes more pronounced when approaching 500Hz due to an increase in both modeled scattering coefficient and simulated scattering behavior for the simplified and full QRD scenarios. The sharp decrease in reverberation time to just above that of the empty room, for frequency ranges above 500Hz, is due to the absorption characteristic of the room. The difference between the results obtained for the simplified and full QRD is because of an under-resolved ray field and a difference in modeling method. Unfortunately, there is no visible result convergence for the full QRD scenario, as can be seen in figure 5b. It is therefore not possible to quantify the difference in results due to the choice simplified modeling or simulating the full QRD geometry. The high number of rays and computation time required to fully resolve the full QRD geometry makes this method ill-suited for integration within the design procedure. The simplified model is on average 2.5 times faster (in this particular scenario) with the same number of rays. Given that the simplified QRD scenario provides steady results with only a 1000 rays, makes this method the preferable for cases where a semi-analytical model can be employed. Full integration of either QRD modeling method into an iterative design procedure remains mostly a question of computation time (see figure 5c) and available resources.

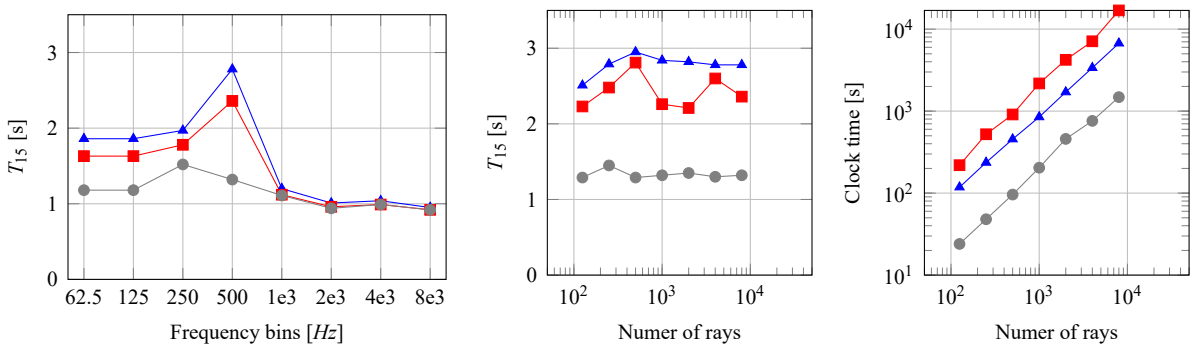

(a) T_{15} values predicted using 8000 rays. (b) T_{15} convergence for 500Hz. (c) Computation times.

Figure 5: Simplified QRD geometry —▲—, full QRD geometry —■— and the room without QRD —●—.

Both the CFD simulations and the acoustic measurements serve to evaluate the predictive power of the LLM models. Unfortunately, both investigations remain unfortunately inconclusive. Figure 6 shows the absorption curves obtained with the LLM methods. The model corrected for the presence of thermal and viscous boundary layers (LLM$_c$) predict a maximum absorption coefficient near 100Hz. This will be corroborated by the acoustical

measurements as shown later. The LLM prediction without correction (LLM_i) predicts peak absorption at a higher frequency as is expected. The CFD results predict a peak near $88Hz$. Assuming the deviation between these predictions to be solely due to a under-prediction of the inertial attached length, a new curve can be fitted to the CFD data. Assuming the attached length to be $2.3d_0$ produces the dotted curve shown in figure 6. The assumption that the asymmetry of the cavity would have little to no impact on the frequency has proved hard to validate. There is a very slight curvature to the temporally averaged air streams that enter the cavity, but this is only slightly noticeable at multiple neck lengths away from the neck at very low velocity compared to the air velocity in the neck.

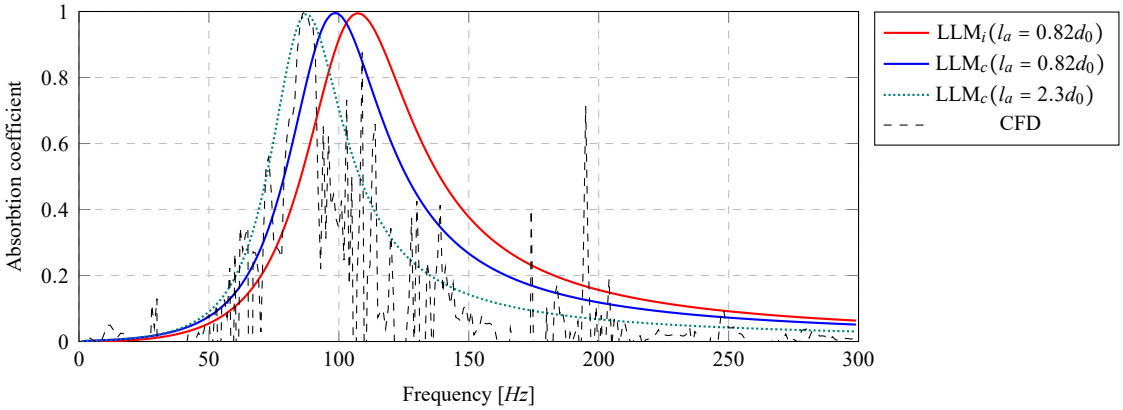

Figure 6: Obtained absorption curves.

The data obtained with the acoustical measurement could not be used to construct an absorption spectrum, however the reverberation times do provide some insight into the resonant frequency of the absorber. Figure 7a shows the relative T_{20} values, measured near one the of the resonator slits. Unfortunately, the first resonator did not produce results that could be separated from the background data, while the resonator (whose results are shown) had a geometrical deviation (as disscused in section 7). The T_{20} values are presented relative to those of the empty test chamber as the T_{20} values of the empty chamber are not uniform across the frequency spec-

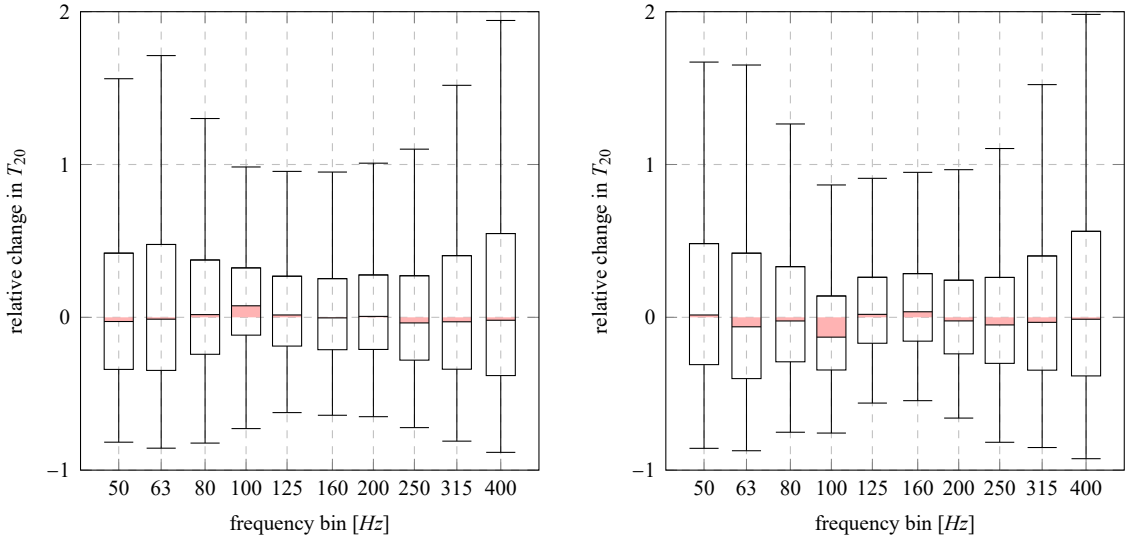

(a) Mic located near 2nd Helmholtz resonator. (b) Mic located at $1m$ distance on symmetry plane.

Figure 7: Relative change in T_{20} with respect to empty room.

trum. There is a small yet defined increase in relative T_{20} at $100Hz$, this should correspond to some continued oscillation of mass in the resonator neck after excitation. The opposite behavior is observed at $1m$ distance from the resonator which would indicate the absorption of sound in that frequency range (see figure 7b). Note that although both these results seem to corroborate the corrected LLM model using an inertial attached length of $0.82d_0$, the fact that the these results are from the resonator with the construction deviation, means that these values might be $\approx 12Hz$ above the expected frequency. This seems to agree with the aforementioned results obtained from the CFD simulations. Since the changes in relative T_{20} are fairly small, especially when compared to the spread of the measurement data and the low resolution across the frequency spectrum, there is no way to either corroborate any conclusion with certainty. It is also not possible to make any meaningful distinction between the corrected and uncorrected model given the acoustical measurements.

9 Conclusions

The proposed design procedure enables the generation of scalable QRD's with internal Helmholtz resonators where an algorithmic solver can control geometry parameters in order to achieve a target resonance frequency. An approximation of the effect of the QRD can be made using Pachyderm where results obtained indicate that applying analytically derived coefficients to larger, simplified surfaces greatly reduces computational time when compared to fully modeled geometry. Simulations using fully modeled geometry show greater deviations in results obtained. However, the similarities between values found using either method could indicate a capability of roughly estimating the effect of other diffusing geometries when analytical models are absent. The absorption spectrum obtained using computational fluid dynamics agrees well with the spectra obtained using the LLM models, after adjusting the inertial attached length. The applicability of the obtained results to other slit resonators remains unknown. The authors would recommend a comprehensive study into the inertial attached lengths for semi-infinite slit resonators. A prototype was evaluated by measuring reverberation times in a reverberation chamber. Data obtained can be interpreted as indicating that the resonance frequencies of the Helmholtz resonators are in reasonable agreement with the predicted frequency. There seems to be disagreement between the resonant frequencies predicted by the CFD modeling and the measurements obtained in the reverberation chamber. This is likely due to a small deviation from the design specifications. The expected frequency shift from this deviation seems to match in magnitude with the disagreement between measurement data and CFD results. Future research should include testing the resonance frequency and absorption coefficient of the Helmholtz resonators using the impedance tube method. The effect of the diffuser and scattering coefficients obtained using Pachyderm should compared with empirical data. Extra effort can be made to investigate the effect geometric deviations occurring in objects made using additive manufacturing on acoustic behavior in comparison to smooth walled objects.

Acknowledgments

The authors would like to thank Arthur van der Harten of Orase for his reflections on the usage of Pachyderm, Efren Fernandez Grande of DTU for his guidance, and Pieter Vreede and Sven Evers of Merford for providing access to their lab and the reverberation time measurements.

References

[1] Kleiner, M.; Tichy, J. *Acoustics of small rooms*. CRC Press, London, 1st edition, 2014.

[2] Wortman, T. Genetic evolution vs. function approximation: Benchmarking algorithms for architectural design optimization. *Journal of Computational Design and Engineering*, 2019. volume 6 (3), pp. 414–428.

[3] Cox, T. J.; D'Antonio, P. *Acoustic Absorbers and Diffusers,Theory, Design and Application*. CRC Press, Londen, 3rd edition, 2017.

[4] Wu, T.; Cox, T.; Lam, Y. From a profiled diffuser to an optimized absorber. *The Journal of the Acoustical Society of America*, 2000. volume 108, pp. 643–50.

[5] Pilch, T.; Kamisinsky, T. The effect of geometrical and material modification of sound diffusers on their acoustic parameters. *Archives of Acoustics*, 2011. volume 36 (4), p. 955–966.

[6] Komkin, A.; Mironov, M.; Bykov, A. Sound absorption by a helmholtz resonator. *Acoustical Physics*, 2017. volume 63, pp. 385–392.

[7] Komkin, A.; Mironov, M.; Yudin, S. On the attached length of orifices. *Acoustical Physics*, 2012. volume 58.

[8] Strutt, J. W.; Rayleigh, B. *The Theory of Sound*, volume 2. Macmillan and Co., LTD, New York, 2nd edition, 1896.

[9] Ingard, U. On the theory and design of acoustic resonators. *Journal of the Acoustical Society of America*, 1953. volume 25, pp. 1037–1061.

[10] Jaouen, L.; Chevillotte, F. Length correction of 2d discontinuities or perforations at large wavelengths and for linear acoustics. *Acta Acustica united with Acustica*, 2018. volume 104 (2), p. 243–250.

[11] Herrero-Durá, I.; Cebrecos, A.; Picó, R.; Romero-García, V.; García-Raffi, L. M.; Sánchez-Morcillo, V. J. Sound absorption and diffusion by 2d arrays of helmholtz resonators. *Journal of Applied Sciences*, 2020. volume 10.

[12] Chanaud, R. Effects of geometry on the resonance frequency of helmholtz resonators. *Journal of Sound and Vibration*, 1994. volume 178 (3), pp. 337–348.